Table 1
Comparison of the theoretical value (Δm_{Au}^{th}) with the practical one (Δm_{Au}^{pr}) for gold electrode

Electrode	Scan rate, mV·s^{-1}	Q, 10^{-3} C	-Δf, Hz	m_{pr}, 10^{-6} g	m_{th}, 10^{-6} g	CE, %	n
	5	4.28	645.82	2.86	2.91	98.28	2.98
	10	2.53	388.41	1.73	1.83	99.83	2.99
Gold	20	1.68	250.71	1.11	1.14	97.36	2.97
	40	1.03	158.31	0.70	0.70	99.85	2.99
	50	9.57	146.79	0.65	0.65	99.84	2.99

Based on the known number of electrons, the current efficiencies (CE) of the gold electrodeposition process were calculated and presented below.

When the potential stepped from 0.95 V (a value where no Au is deposited on the gold electrode surface) to +0.7 V, the average change in frequency was measured as being 645.82 Hz. Using Sauerbrey's Eq. (1), the change in frequency can be correlated to the change in mass. Comparing the theoretical value (Δm_{Au}^{th}) with the experimental one (Δm_{Au}^{exp}), a very good agreement can be seen (Table 1).

The recorded cyclic voltammetry for gold electrodes at different scanning rates from 5 mV·s^{-1} to 50 mV·s^{-1} is shown in Fig. 2. The inserted plot shows the dependence of the peak of the cathodic current on the square root of the scan rate.

It is seen in the figure that an increase in the cathode current (j_{pc}) coincides with an increase in the potential scan rate (v). This dependence is described by the Randles- Ševčik equation, while the linear dependence j_{pc} vs. v$^{1/2}$ (Fig. 2) indicates the diffusion limitation of this process. From the slope of the linear dependence, the diffusion coefficient of ions $AuCl_4^-$ in the solution was calculated to be equal to $1.6 \cdot 10^{-5}$ cm^2·s^{-1}.

Fig. 3. Cyclic voltammograms on carbon electrode in black curve – 0.1 M HCl + 100 mg·L^{-1} HAuCl$_4$ and red curve – 0.1 M HCl at 5 mV· s^{-1}.

3.2. Electroreduction of gold on a carbon electrode

Cyclic voltammetry was performed on carbon-capped electrodes, and as can be seen in Fig. 3 (black curve) this resulted in an oxidative peak (0.80 V) in the reverse scan and a reductive peak (0.55 V) in the forward scan. In the background electrolyte 0.1 M HCl, a carbon electrode was also examined in this potential region (Fig. 3, red curve). However, no clear redox processes were observed. Since CARH has a large surface area, large charge-discharge currents of the double electric layer (non-Faraday currents) were revealed on the voltammogram. Thereby in order to calculate the kinetic data on the gold electroreduction reaction on this material, compensation should be made for a non-Faraday current.

For this purpose, the currents of a double electric layer (Fig. 3, red curve) were taken from the value of the cathodic current peak (Fig. 3, black curve). Finally, the resulting peak current values – j_{pc} were used to calculate the diffusion coefficient. Figure 4a illustrates cyclic voltammograms of the background electrolyte, which were used subsequently to compensate for non-Faraday currents.
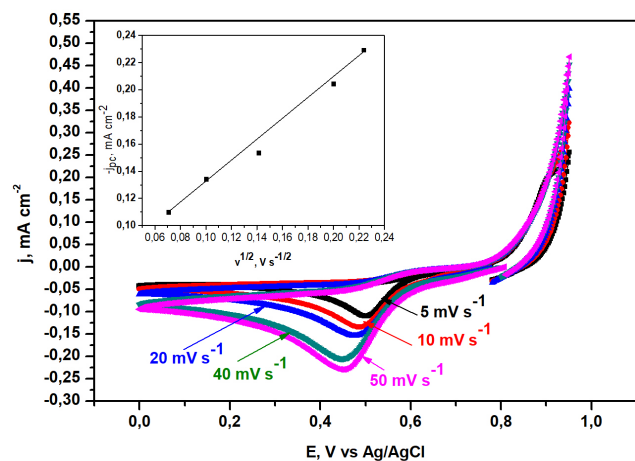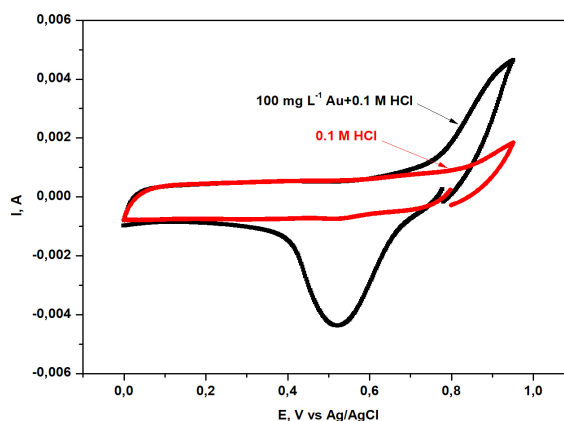

Fig. 2. Cyclic voltammograms for a gold quartz-crystal in 100 mg·L^{-1} HAuCl$_4$ solution of various scan rates: 5, 10, 20, 40 and 50 mV·s^{-1}.